Counterion Effects in Pd Polyselenides: Evolution from Molecular to Three-Dimensional Framework Structures

Kang-Woo Kim and Mercouri G. Kanatzidis*

Contribution from the Department of Chemistry and the Center for Fundamental Materials Research, Michigan State University, East Lansing, Michigan 48824

Received April 16, 1998

Abstract: Several palladium polyselenides were prepared by the reactions of Pd^{2+} ions with Se_x^{2-} ($4 < x < 6$) ligands in the presence of various cations. $\{(CH_3)N(CH_2CH_2)_3N\}_2[Pd(Se_6)_2]$ (**I**) was prepared by the methanothermal reaction of K_2PdCl_4, K_2Se_4, and $\{(CH_3)_3N(CH_2CH_2)N(CH_3)_3\}I_2$ in a 1:3:2 molar ratio at 110 °C. Compound **I** crystallizes in the space group $P2_1/c$ with $a = 9.403(3)$ Å, $b = 15.050(5)$ Å, $c = 10.807(4)$ Å, $\beta = 91.73(3)°$, and $V = 1528.7(9)$ Å^3. $(H_3NCH_2CH_2NH_2)_2[Pd(Se_5)_2]$ (**II**) was prepared by the methanothermal reaction of $PdCl_2$, Na_2Se_4, and $(H_3NCH_2CH_2NH_3)Cl_2$ in a 1:3:1 molar ratio at 80 °C. Compound **II** crystallizes in the space group $P2_1/n$ with $a = 9.412(3)$ Å, $b = 8.671(3)$ Å, $c = 12.666(3)$ Å, $\beta = 98.38(2)°$, and $V = 1023(1)$ Å^3. The anions in $[Pd(Se_5)_2]^{2-}$ in **II** and $[Pd(Se_6)_2]^{2-}$ in **I** are polymeric and possess layered structures. The organic cations are located between the layers. $K_2(H_3NCH_2CH_2NH_3)_2[Pd(Se_4)_2{\cdot}2Se_4]$ (**III**) was prepared by the methanothermal reaction of $PdCl_2$, K_2Se_4, and $(H_3NCH_2CH_2NH_3)Cl_2$ in a 1:3:1 molar ratio at 80 °C. Compound **III** crystallizes in the space group $I2_12_12_1$ with $a = 12.587(9)$ Å, $b = 15.271(5)$ Å, $c = 15.404(9)$ Å, and $V = 2961(5)$ Å^3. The $[Pd(Se_4)_2{\cdot}2Se_4]^{6-}$ anion in **III** is composed of a $[Pd(Se_4)_2]^{2-}$ three-dimensional adamantane-like framework with large cavities that are filled with the counterions and with uncoordinated Se_4^{2-} ligands. $K_6[Pd(Se_5)_4]$ (**IV**) was prepared by the methanothermal reaction of K_2PdCl_4 and K_2Se_5 in a 1:6 molar ratio at 80 °C. The black polyhedral crystals of **IV** are slightly soluble in water. Compound **IV** crystallizes in the space group *Pbcn* with $a = 12.427(4)$ Å, $b = 13.777(9)$ Å, $c = 19.190(9)$ Å, and $V = 3285(5)$ Å^3. The $[Pd(Se_5)_4]^{6-}$ anion is molecular and one of the most Se-rich metal polyselenides known. It has a palladium center with four dangling Se_5^{2-} ligands around it. Being a molecular fragment, it can be regarded as a building block for extended $[Pd(Se_n)_2]^{2-}$ frameworks. Optical spectroscopic and thermal gravimetric analysis data for the compounds are reported.

Introduction

Structure-directing effects of various cations are often encountered in the synthesis of zeolites and other microporous framework materials.[1] The effect, however, is general, and it is well manifested in the area of metal chalcogenide and polychalcogenide chemistry.[2] Such effects can be exploited to direct the synthesis of solids toward a desired dimensionality, for example the deliberate synthesis of three-dimensional (3-D) framework solids or two-dimensional (2-D) and one-dimensional (1-D), even discrete cluster (0-D), entities all with the same framework composition but with different counterion templates. It appears that in most cases, the structure-directing effect of a counterion is predictable; the smaller the counterion, the higher the dimensionality of the accompanying framework is. This statement applies only if the stoichiometry of the counteranion does not change (i.e., from cation to cation) or changes very little. Outstanding examples of the counterion effect are many in the literature. Noteworthy of mention are $(Ph_4P)_2Au_2(Se_x)_2$ ($x = 2-4$) and $Cs_2Au_2(Se_3)_2$,[3] ACuTe[4] and AAuTe[5] (A = Na, K, or Cs), $(Ph_4P)M(Se_6)_2$ (M = Ga, In, or Tl)[6] and the series $(Ph_4P)Ag(Se_4)$,[7] $(Me_4N)Ag(Se_5)$,[8] α-$KCuS_4$,[9] $CsCuS_6$,[10] $[(Et_4N)Ag(Se_4)]_4$,[11] and $(Me_4N)[Ag(Te_4)]$.[12] In these systems a clear trend exists where smaller counterions stabilize higher dimensional structures and favor higher coordination numbers in the framework atoms when possible. Another such system seems to be $(Ph_4P)_2[PdSe_8]$[13] and K_2PdSe_{10},[14] where the former compound has a discrete molecular coordination complex in its lattice while the latter features the same $[PdSe_8]^{2-}$ anion polymerized in three dimensions. The decrease in cation size in going from Ph_4P^+ to K^+ is enormous and, remarkably, causes

(1) (a) Davis, M. E. *CHEMTECH* **1994**, *24*, 22−26. (b) Thomas, J. M. *Z. Phys. Chem.* **1996**, *197*, 37−48. (c) Lewis, D. W.; Sankar, G.; Wyles, J. K.; Thomas, J. M.; Catlow, C. R. A.; Willock, D. J. *Angew. Chem., Int. Ed. Engl*. **1997**, *36*, 2675−2677. (d) Oliver, S.; Kuperman, A.; Ozin, G. A. *Angew. Chem., Int. Ed. Engl*. **1998**, *37*, 46−62 and references therein.

(2) Kanatzidis M. G. *Phosphorous, Sulfur Silicon Relat. Elem.* **1994**, *93*−*94*, 159.

(3) (a) Huang, S.-P.; Kanatzidis, M. G. *Coord. Chem. Rev*. **1994**, *130*, 509. (b) Park, Y.; Kanatzidis, M. G. *J. Alloys Compd.* **1997**, *257*, 137−145.

(4) (a) Berger, R.; Eriksson, L. *J. Less-Common Met.* **1990**, *161*, 101. (b) Savelsberg, G.; Schäfer, H. *Z. Naturforsch.* **1978**, *33B*, 370.

(5) Bronger, W.; Kathage, H. U. *J. Alloys Compd*. **1992**, *184*, 87.

(6) Dhingra, S.; Kanatzidis M. G. *Science* **1992**, *258*, 1769−1772.

(7) Kanatzidis, M. G.; Huang, S.-P. *J. Am. Chem. Soc.* **1989**, *111*, 760−761.

(8) Banda, R. M. H.; Craig, D. C.; Dance, I. G.; Scudder, M. L. *Polyhedron* **1989**, *8*, 2379−2383.

(9) (a) Kanatzidis, M. G.; Park, Y. *J. Am. Chem. Soc.* **1989**, *111*, 3767. (b) Park, Y. Ph.D. Thesis, Michigan State University, 1992.

(10) McCarthy, T.; Zhang, X.; Kanatzidis, M. G. *Inorg. Chem.* **1993**, *32*, 2944−2948.

(11) Huang, S.-P.; Kanatzidis, M. G. *Inorg. Chem.* **1991**, *30*, 1455−1466.

(12) Kim, K.-W.; Kanatzidis, M. G. *J. Am. Chem. Soc.* **1993**, *115*, 5871.

(13) (a) Käuter, G.; Dehnicke, K. *Chem.-Ztg* **1990**, *114*, 7−9. (b) Adams, R. D.; Wolfe, T. A.; Eichhorn, B. W.; Haushalter, R. C. *Polyhedron* **1989**, *8*, 701−703. (c) Kim, K.-W.; Kanatzidis, M. G. *Inorg. Chem.* **1993**, *32*, 4161−4163.

(14) Kim, K.-W.; Kanatzidis, M. G. *J. Am. Chem. Soc.* **1992**, *114*, 4878.

S0002-7863(98)01297-9 CCC: $15.00
Published on Web 08/05/1998

Chart 1. Schematic of Framework Materials[a]

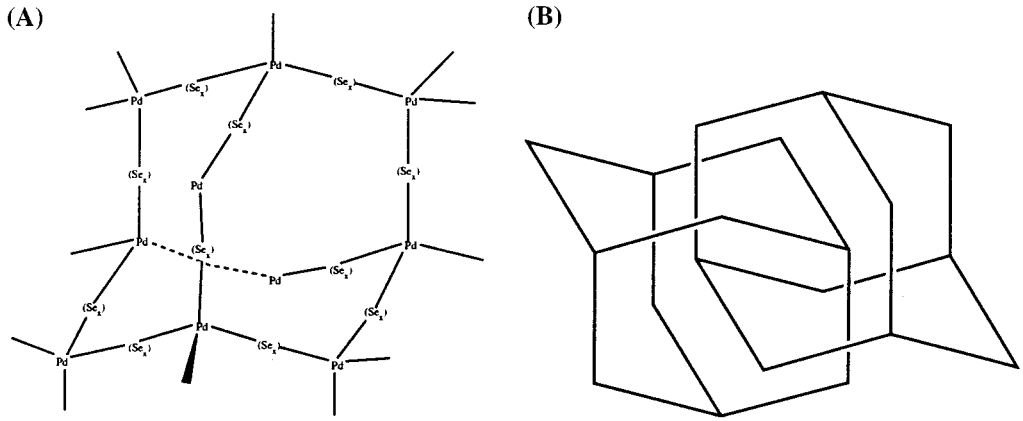

[a] (A) Schematic representation of a single 3-D framework of $[Pd(Se_x)_2]^{2-}$. The tetrahedral depiction of Pd atoms signifies the disposition and connectivity pattern of the Se_x^{2-} ligands, not their actual coordination geometry, which is square planar. (B) Interpenetrating behavior of $[Pd(Se_4)_2]^{2-}$ and $[Pd(Se_6)_2]^{2-}$ frameworks.

K_2PdSe_{10} to form two interpenetrating 3-D frameworks, namely, $[PdSe_8]^{2-}$ and $[PdSe_{12}]^{2-}$. Therefore, $K_4[Pd(Se_4)_2][Pd(Se_6)_2]$ is a more descriptive formulation. Both frameworks adopt diamond-like topologies. Shown in Chart 1, the individual $[Pd(Se_x)_2]^{2-}$ frameworks are *topologically* equivalent[15] to the structure of cristobalite SiO_2 (Pd^{2+} atoms occupy the Si sites and Se_x^{2-} ligands occupy the O sites). There are no covalent or ionic bonds between these two frameworks, and thus one can never cross, through bonds, from one to the other.

To stabilize one of the frameworks separately from the other, we investigated cations intermediate in size between Ph_4P^+ and K^+, for example, $[H_3NCH_2CH_2NH_2]^+$ and $[(CH_3)N(CH_2CH_2)_3N(CH_3)]^{2+}$. The latter is a dication and so, per single charge, only half of its true size could be considered. We reasoned that these cations would be small enough to cause bonding associations between the various discrete $[PdSe_8]^{2-}$ or $[PdSe_{10}]^{2-}$ anions to form a polymeric structure but would be too large to allow interpenetration of the two frameworks as it happens in the K^+ salt. To achieve this, we applied the hydro(solvo)thermal synthetic method, which is proven to be very effective for the synthesis of such compounds.[16] One related notable compound is $(NH_4)_2[PdS_{11}]$,[17] which was reported to have a polymeric structure containing disordered S_5^{2-} and S_6^{2-} ligands. A salient feature of this compound is that it has a small counterion that is probably responsible for its structural departure from the typical molecular motif. Unfortunately, the disorder among the various sulfur atoms precludes one from unequivocally deciding whether the compound is layered or three-dimensional.

Here we report on several new derivatives of the palladium polyselenide system that indeed feature new frameworks whose dimensionality has been directed by the operating counterions. Namely, we report on $\{(CH_3)N(CH_2CH_2)_3N\}_2[Pd(Se_6)_2]$, $(H_3NCH_2CH_2NH_2)_2[Pd(Se_5)_2]$, and $K_2[(H_3NCH_2CH_2NH_3)_2[Pd(Se_4)_2\cdot 2Se_4]$. Finally, we also describe the K^+ salt of the striking, discrete molecular complex $[Pd(Se_5)_4]^{6-}$, which may very well be the common precursor to all polymeric palladium polyselenides. With $(Ph_4P)_2[PdSe_8]$ and K_2PdSe_{10},[14] and the systems described here, we now have an interesting set of compounds, with similar stoichiometries, which illustrate in a rather spectacular sense the role of counterions in stabilizing molecular versus extended structures.

Experimental Section

Reagents. The chemicals in this research were used as obtained without further purification. K_2Se_4 and K_2Se_5 were prepared by dissolving the stoichiometric amount of potassium metal and elemental selenium in liquid ammonia. $PdCl_2$ and K_2PdCl_4 were from Alfa. 1,4-Diazabicyclo[2.2.2]octane was from Aldrich. Methyl iodide (98%) and ethylenediamine were from J. T. Baker. MeOH was distilled after refluxing over CaH_2. Diethyl ether was distilled after refluxing over potassium metal in the presence of benzophenone and triethyleneglycol−dimethyl ether for several hours.

Synthesis. All experiments and manipulations were performed under an atmosphere of dry nitrogen using either a vacuum atmosphere Dri-Lab glovebox or a Schlenk line.

$(H_3NCH_2CH_2NH_2)_2[Pd(Se_5)_2]$ (I). Amounts of 0.030 g (0.17 mmol) of $PdCl_2$, 0.184 g (0.51 mmol) of Na_2Se_4, 0.023 g (0.17 mmol) of $H_3NCH_2CH_2NH_3Cl_2$, and 0.4 mL of methanol were charged in a Pyrex tube. The tube was sealed off under vacuum and heated at 80 °C for 3 days. Black hexagonal platelet crystals (49% yield) were isolated by filtration and washed with methanol several times. These crystals are insoluble in water and most organic solvents. Semiquantitative analysis by the scanning electron microscopy/energy-dispersive spectrometry (SEM/EDS) technique showed the Pd/Se atomic ratio as 1.0:8.8.

$\{(CH_3)N(CH_2CH_2)_3N\}_2[Pd(Se_6)_2]$ (II). Amounts of 0.040 g (0.12 mmol) of K_2PdCl_4, 0.145 g (0.37 mmol) of K_2Se_4, 0.097 g (0.24 mmol) of $\{(CH_3)N(CH_2CH_2)_3N(CH_3)\}I_2$, and 0.5 mL of methanol were charged in a Pyrex tube. The tube was sealed off under vacuum and heated at 110 °C for 5 days. Black rectangular rod crystals (25% yield) were isolated by filtration and washed with methanol several times. These crystals are insoluble in water and most organic solvents. Semiquantitative analysis by the SEM/EDS technique showed the Pd/Se atomic ratio as 1.0:12.2.

$K_2[(H_3NCH_2CH_2NH_3)_2[Pd(Se_4)_2\cdot 2Se_4]$ (III). Amounts of 0.040 g (0.23 mmol) of $PdCl_2$, 0.266 g (0.68 mmol) of K_2Se_4, 0.030 g (0.23 mmol) of $H_3NCH_2CH_2NH_3Cl_2$, and 0.4 mL of methanol were charged in a Pyrex tube. The tube was sealed off under vacuum and heated at

(15) The analogy to diamond and SiO_2 is strictly topological. It is not meant to say that the local coordination of Pd is close to being tetrahedral. The structures in Chart 1 were drawn by ignoring the polyselenide ligands and connecting the Pd atoms in space.

(16) (a) Liao, J.-H.; Kanatzidis, M. G. *Inorg. Chem.* **1992**, *31*, 431−439. (b) Liao, L. H.; Kanatzidis, M. G. *J. Am. Chem. Soc.* **1990**, *112*, 7400−7402. (c) Huang, S.-P.; Kanatzidis, M. G. *J. Am. Chem. Soc.* **1992**, *114*, 5477−5478. (d) Sheldrick, W. S. *Z. Anorg. Allg. Chem.* **1988**, *562*, 23−30. (e) Sheldrick, W. S.; Hauser, H.-J. *Z. Anorg. Allg. Chem.* **1988**, *557*, 98−104. (f) Sheldrick, W. S.; Hauser, H.-J. *Z. Anorg. Allg. Chem.* **1988**, *557*, 105−110. (g) Wood, P. T.; Pennington, W. T.; Kolis, J. W. *Inorg. Chem.* **1993**, *32*, 129−130. (h) Wood, P. T.; Pennington, W. T.; Kolis, J. W. *J. Chem. Soc., Chem. Commun.* **1993**, *25*, 235−236. (i) Chou, J.-H.; Kanatzidis, M. G. *Inorg. Chem.* **1994**, *33*, 1001−1002. (j) Chou, J.-H.; Kanatzidis, M. G. *Chem. Mater.* **1995**, *7*, 5−8. (k) Chou, J.-H.; Kanatzidis, M. G. *J. Solid State Chem.* **1996**, *123*, 115−122.

(17) (a) Haradem, P. S.; Cronin, J. L.; Krause, R. L.; Katz, L. *Inorg. Chim. Acta* **1977**, *25*, 173−179 and references therein. (b) Wickenden, A. E.; Krause, R. A. *Inorg. Chem.* **1969**, *8*, 779−783.

80 °C for 3 days. Black octahedral chunky crystals (54% yield) were isolated by filtration and washed with methanol several times. These crystals are insoluble in water and most organic solvents and decompose gradually in water. Semiquantitative analysis by the SEM/EDS technique showed the K/Pd/Se atomic ratio as 1.9:1.0:14.8.

$K_6[Pd(Se_5)_4]$ (IV). Amounts of 0.040 g (0.12 mmol) of K_2PdCl_4, 0.348 g (0.74 mmol) of K_2Se_5, and 0.5 mL of methanol were charged in a Pyrex tube. The tube was sealed off under vacuum and heated at 80 °C for 2 days. Black polyhedral crystals (43% yield) were isolated by filtration and washed with methanol several times. These crystals are slightly soluble in water. Semiquantitative analysis by the SEM/EDS technique showed the K/Pd/Se atomic ratio as 4.7:1.0:18.1.

Physicochemical Methods. UV−vis−near-IR diffuse reflectance spectra were obtained on a Shimadzu UV-3101PC double-beam, double-monochromator spectrophotometer in the wavelength range of 200−2500 nm. $BaSO_4$ powder was used as a reference and base material, on which the ground powder sample was coated. Reflectance data were converted to absorbance data as described elsewhere.[18] The band-gap energy value was determined by extrapolation from the linear portion of the absorption edge in a (α/S) versus E plot. Semiquantitative analyses of the compounds were done by SEM/EDS as described previously.[19] Thermal gravimetric analysis (TGA) was performed on a Shimadzu TGA-50. The samples were heated to 800 °C at a rate of 5 or 10 °C/min under a steady flow of dry N_2 gas.

X-ray Crystallographic Studies. A single crystal of each compound, **I**−**IV**, was mounted on the tip of a glass fiber with epoxy adhesive and coated with Krylon to protect it from prolonged exposure to air. The crystallographic data for **I**, **III**, and **IV** were collected on Rigaku AFC6S four-circle automated diffractometers at room temperature. The data for **II** were collected on a Nicolet P3 four-circle automated diffractometer at −120 °C. Accurate unit cell parameters were determined from the 2θ, ω, ϕ, and χ angles of 15−25 machine-centered reflections. The intensities of three standard reflections were checked every 100 or 150 reflections to monitor crystal and instrument stability. No appreciable decay was observed during the data collection period. An empirical absorption correction based on ψ scans of three strong reflections with $\chi \sim 90°$ was applied to each data set. The structures were solved with direct methods using the SHELXS-86 software program[20] and refined with full-matrix least-squares techniques. After isotropic refinement of all atoms, a DIFABS correction was applied.[21] All calculations were performed on a VAXstation 3100/76 computer using the TEXSAN crystallographic software package from Molecular Structure Corp.[22]

All non-hydrogen and non-carbon atoms in **I**−**IV** were refined anisotropically. Hydrogen atom positions were calculated but not refined.

Tables 1 and 2 show the crystal data and details for the structure analysis of all compounds. The fractional coordinates and temperature factors (B_{eq}) of all atoms with their estimated standard deviations are given in Tables 3−6.

X-ray powder diffraction (XRD) patterns were obtained with a Rigaku-Denki/RW400F2 (Rotaflex) rotating anode powder diffractometer. Ni-filtered Cu radiation was used operating at 45 kV and 100 mA. The crystals of each compound were ground to powder and put on a glass slide using double-sided sticky tape. On the basis of the atomic coordinates from the X-ray single-crystal diffraction study, X-ray powder patterns for all compounds were calculated with the software package CERIUS.[23] The observed X-ray powder patterns were in good agreement with those calculated, ensuring the homogeneity and purity of the compounds. Calculated and observed X-ray powder patterns showing d spacings and intensities of the strongest hkl reflections are given in the Supporting Information.

Table 1. Summary of Crystallographic Data for $\{(CH_3)N(CH_2CH_2)_3N\}_2[Pd(Se_6)_2]$ (**I**) and $(H_3NCH_2CH_2NH_2)_2[Pd(Se_5)_2]$ (**II**)

	(**I**)	(**II**)
formula	$C_{12}H_{14}N_4PdSe_{12}$	$C_4H_{18}N_4PdSe_{10}$
fw	1308.34	1018.21
crystal shape	rectangular rod	hexagonal platelet
crystal color	black	black
crystal size (mm)	0.05 × 0.08 × 0.13	0.06 × 0.10 × 0.14
temperature (°C)	23	23
crystal system	monoclinic	monoclinic
space group	$P2_1/c$ (no. 14)	$P2_1/n$ (no. 14)
a (Å)	9.403(3)	9.412(3)
b (Å)	15.050(5)	8.671(3)
c (Å)	10.807(4)	12.666(3)
α (deg)	90	90
β (deg)	91.73(3)	98.38(2)
γ (deg)	90	90
V (Å^3), Z	1529(1), 2	1023(1), 2
μ (cm^{-1}) Mo Kα	147.61	185.15
d_{calc} (g/cm^3)	2.842	3.307
scan method	$\omega/(2\theta)$	$\omega/(2\theta)$
$2\theta_{max}$ (deg)	45	50
no. of reflections collected	2243	2062
no. of reflections, $F_o^2 > 3\sigma(F_o)^2$	954	853
no. of variables	107	88
max shift/esd	0.00	0.00
phasing method	direct methods	direct methods
R/R_w (%)[a]	3.8/4.0	3.6/3.8

[a] $R = \sum||F_o| - |F_c||/\sum|F_o|$. [b] $R_w = \{\sum w(|F_o| - |F_c|)^2/\sum w|F_o|^2\}^{1/2}$.

Table 2. Summary of Crystallographic Data for $K_2(H_3NCH_2CH_2NH_3)_2[Pd(Se_4)_2{\cdot}2Se_4]$ (**III**) and $K_6[Pd(Se_5)_4]$ (**IV**)

	(**III**)	(**IV**)
formula	$C_4H_{20}N_4K_2PdSe_{16}$	K_6PdSe_{20}
fw	1572.19	1920.19
crystal shape	octahedral chunk	polyhedral chunk
crystal color	black	black
crystal size (mm)	0.16 × 0.20 × 0.24	0.10 × 0.28 × 0.32
temperature (°C)	−120	23
crystal system	orthorhombic	orthorhombic
space group	$I2_12_12_1$ (no. 24)	$Pbcn$ (no. 60)
a (Å)	12.587(9)	12.427(4)
b (Å)	15.271(5)	13.777(9)
c (Å)	15.404(9)	19.190(9)
α (deg)	90	90
β (deg)	90	90
γ (deg)	90	90
V (Å^3), Z	2961(5), 4	3285(5), 4
μ (cm^{-1}) Mo Kα	203.88	232.64
d_{calc} (g/cm^3)	3.527	3.882
scan method	$\omega/(2\theta)$	$\omega/(2\theta)$
$2\theta_{max}$ (deg)	45	50
no. of reflections collected	1878	2458
no. of reflections, $F_o^2 > 3\sigma(F_o)^2$	885	842
no. of variables	109	127
max shift/esd	0.00	0.00
phasing method	direct methods	direct methods
R/R_w (%)[a]	5.5/5.0	6.2/7.6

[a] $R = \sum||F_o| - |F_c||/\sum|F_o|$. [b] $R_w = \{\sum w(|F_o| - |F_c|)^2/\sum w|F_o|^2\}^{1/2}$.

Results and Discussion

The successful isolation of the three polymeric polyselenides $\{(CH_3)N(CH_2CH_2)_3N\}_2[Pd(Se_6)_2]$ (**I**), $(H_3NCH_2CH_2NH_2)_2[Pd(Se_5)_2]$ (**II**), and $K_2[(H_3NCH_2CH_2NH_3)_2[Pd(Se_4)_2{\cdot}2Se_4]$ (**III**), all with different anion structures, attests, without a doubt, that there is a strong templating counterion effect in the cation/Pd/Se_x system. Therefore, the stability of the anionic Pd/Se_x entity depends strongly on steric factors and very little on electronic

(18) Zhang, X.; Kanatzidis, M. G. *J. Am. Chem. Soc.* **1994**, *116*, 1890.
(19) Sutorik, A. C.; Albritton-Thomas, J.; Kannewurf, C. R.; Kanatzidis, M. G. *J. Am. Chem. Soc.* **1994**, *116*, 7706−7713.
(20) Sheldrick, G. M. In *Crystallographic Computing 3*; Sheldrick, G. M., Kruger, C., Goddard, R., Eds.; Oxford University Press: Oxford, U.K., 1985; pp 175−189.
(21) Walker, N.; Stuart, D. An Empirical Method for Correcting Diffractometer Data for Absorption Effects. *Acta Crystallogr.* **1983**, *A39*, 158.
(22) *TEXSAN: Single-Crystal Structure Analysis Software*, version 5.0; Molecular Structure Corporation: The Woodlands, TX, 1994.
(23) *CERIUS*^{2}, Version 2.0; Molecular Simulations Inc.: Cambridge, U.K., 1995.

Table 3. Fractional Atomic Coordinates and B_{eq} Values for $\{(CH_3)N(CH_2CH_2)_3N\}_2[Pd(Se_6)_2]$ (**I**)[a]

atom	*x*	*y*	*z*	B_{eq} (Å^2)[b]
Pd	0	0	0	2.0(1)
Se(1)	−0.2021(2)	0.0719(1)	0.0998(2)	2.8(1)
Se(2)	−0.2454(2)	0.0108(1)	0.2944(2)	3.2(1)
Se(3)	−0.0917(2)	0.0843(2)	0.4353(2)	3.5(1)
Se(4)	0.2017(2)	−0.2872(1)	−0.0066(2)	3.4(1)
Se(5)	0.2266(2)	−0.1878(1)	0.1598(2)	3.1(1)
Se(6)	0.0217(2)	−0.1016(1)	0.1763(2)	2.7(1)
N(1)	0.331(2)	0.129(1)	0.249(1)	2.9(8)
N(2)	0.334(2)	0.234(1)	0.062(1)	3.5(9)
C(1)	0.324(3)	0.067(2)	0.359(2)	5.4(6)
C(2)	0.365(2)	0.078(1)	0.133(2)	4.0(5)
C(3)	0.377(2)	0.143(1)	0.030(2)	4.0(5)
C(4)	0.440(2)	0.200(1)	0.270(2)	4.0(5)
C(5)	0.430(2)	0.264(1)	0.165(2)	3.7(5)
C(6)	0.189(2)	0.174(1)	0.231(2)	4.2(5)
C(7)	0.188(2)	0.232(1)	0.112(2)	4.1(5)

[a] Estimated standard deviations in parentheses. [b] Anisotropically refined atoms are given in the form of the isotropic equivalent displacement parameter defined as $B_{eq} = (8\pi^2/3)[a^2B_{11} + b^2B_{22} + c^2B_{33} + ab(\cos\gamma)B_{12} + ac(\cos\beta)B_{13} + bc(\cos\alpha)B_{23}]$. The anisotropic temperature factor expression is $\exp[-2\pi^2(B_{11}a^{*2}h^2 + ... + 2B_{12}a^*b^*hk + ...)]$.

Table 4. Fractional Atomic Coordinates and B_{eq} Values for $(H_3NCH_2CH_2NH_2)_2[Pd(Se_5)_2]$ (**II**)[a]

atom	*x*	*y*	*z*	B_{eq} (Å^2)[b]
Pd	1/2	0	1/2	1.69(7)
Se(1)	0.2561(2)	0.0934(2)	0.4390(1)	2.20(7)
Se(2)	0.0924(2)	−0.1126(2)	0.4234(1)	2.56(8)
Se(3)	0.1675(2)	−0.2559(2)	0.2824(1)	2.53(8)
Se(4)	0.0945(2)	−0.1014(2)	0.1302(1)	2.36(7)
Se(5)	−0.0969(2)	−0.2466(2)	0.0391(1)	2.23(7)
N(1)	0.710(2)	0.082(2)	0.148(1)	6(1)
N(2)	0.540(2)	−0.242(2)	0.276(2)	5(1)
C(1)	0.686(2)	−0.025(2)	0.227(2)	4(1)
C(2)	0.561(2)	−0.139(3)	0.187(2)	5(1)

[a] Estimated standard deviations in parentheses. [b] Anisotropically refined atoms are given in the form of the isotropic equivalent displacement parameter defined as $B_{eq} = (8\pi^2/3)[a^2B_{11} + b^2B_{22} + c^2B_{33} + ab(\cos\gamma)B_{12} + ac(\cos\beta)B_{13} + bc(\cos\alpha)B_{23}]$. The anisotropic temperature factor expression is $\exp[-2\pi^2(B_{11}a^{*2}h^2 + ... + 2B_{12}a^*b^*hk + ...)]$.

ones. As long as the square-planar geometry around the Pd atom is satisfied, any arrangement between Pd^{2+} and Se_x^{2-} is plausible.

Two-Dimensional Systems. The choice of $[(CH_3)N(CH_2CH_2)_3N(CH_3)]^{2+}$ as a counterion was arrived at by careful examination of molecular models of the two independent frameworks of K_2PdSe_{10}, which suggested that if a single framework were to be stabilized, a cation with a volume slightly smaller than Me_4N^+ might work. The dication can be regarded as the product of fusion between two Me_4N^+ cations, as shown in Scheme 1.

It is interesting that $[(CH_3)N(CH_2CH_2)_3N(CH_3)]^{2+}$, which was intended to be incorporated intact, did not survive the synthetic conditions and was demethylated, giving rise to the monocation $[(CH_3)N(CH_2CH_2)_3N]^+$,[24] which of course is larger than even Me_4N^+ on a per-unit-charge basis. The anionic framework in the resulting compound $[(CH_3)N(CH_2CH_2)_3N]_2[Pd(Se_6)_2]$ is two-dimensional; see Figure 1. In contrast, the same anion in K_2PdSe_{10} adopts a three-dimensional diamond-like configuration. The conformations of the Se_6^{2-} chains that serve as bridges between the Pd^{2+} atoms are of the helical screw type. The

(24) The demethylation is the result of nucleophilic attack of the Se_x^{2-} anions on the methyl group of one of the quaternary nitrogen atoms.

Table 5. Fractional Atomic Coordinates and B_{eq} Values for $K_2(H_3NCH_2CH_2NH_3)_2[Pd(Se_4)_2\cdot 2Se_4]$ (**III**)[a]

atom	*x*	*y*	*z*	B_{eq} (Å^2)[b]
Pd	0.1250	1/2	1/4	0.9
Se(1)	0.1330(4)	0.3489(2)	0.3003(2)	1.3(2)
Se(2)	0.0937(4)	0.2523(2)	0.1847(2)	1.3(2)
Se(3)	0.1171(4)	0.4500(2)	0.0986(2)	1.3(2)
Se(4)	0.1561(4)	0.5653(2)	0.0021(3)	1.4(2)
Se(5)	0.2866(4)	0.1992(2)	0.4289(3)	2.0(2)
Se(6)	0.4000(4)	0.0781(2)	0.4368(3)	2.0(2)
Se(7)	0.0372(4)	0.1790(2)	−0.0509(3)	2.1(2)
Se(8)	0.1503(4)	0.1865(2)	−0.1725(3)	1.9(2)
K(1)	0	1/4	0.4533(8)	2.2(6)
K(2)	1/4	0.2952(7)	0	2.0(6)
N(1)	−0.085(3)	0.124(2)	−0.281(2)	3(2)
N(2)	−0.336(3)	0.527(2)	0.630(2)	3(2)
C(1)	−0.087(3)	0.044(2)	−0.227(2)	1.7(7)
C(2)	−0.337(3)	0.472(2)	0.712(2)	1.8(7)

[a] Estimated standard deviations in parentheses. [b] Anisotropically refined atoms are given in the form of the isotropic equivalent displacement parameter defined as $B_{eq} = (8\pi^2/3)[a^2B_{11} + b^2B_{22} + c^2B_{33} + ab(\cos\gamma)B_{12} + ac(\cos\beta)B_{13} + bc(\cos\alpha)B_{23}]$. The anisotropic temperature factor expression is $\exp[-2\pi^2(B_{11}a^{*2}h^2 + ... + 2B_{12}a^*b^*hk + ...)]$.

Table 6. Fractional Atomic Coordinates and B_{eq} Values for $K_6[Pd(Se_5)_4]$ (**IV**)[a]

atom	*x*	*y*	*z*	B_{eq} (Å^2)[b]
Pd	0	1/2	0	1.4(3)
Se(1)	0.0169(4)	0.5177(4)	0.1263(3)	1.6(2)
Se(2)	0.1975(4)	0.4898(4)	0.1608(3)	1.8(2)
Se(3)	0.2577(4)	0.6383(4)	0.2106(3)	2.0(2)
Se(4)	0.3396(4)	0.7354(4)	0.1241(3)	2.2(3)
Se(5)	0.5157(4)	0.6744(4)	0.1204(3)	2.2(3)
Se(6)	0.1939(4)	0.4675(4)	−0.0085(3)	1.9(3)
Se(7)	0.2466(4)	0.4511(4)	−0.1255(3)	2.2(2)
Se(8)	0.2695(4)	0.6112(5)	−0.1727(3)	2.7(3)
Se(9)	0.3869(5)	0.6986(5)	−0.1017(3)	2.9(3)
Se(10)	0.5620(4)	0.6498(4)	−0.1263(3)	2.1(3)
K(1)	1/2	0.486(1)	−1/4	2.1(8)
K(2)	0	0.336(1)	1/4	2.4(9)
K(3)	0	0.696(1)	1/4	3(1)
K(4)	1/2	1/2	0	4(1)
K(5)	0.150(1)	0.707(1)	−0.0011(7)	2.9(6)

[a] Estimated standard deviations in parentheses. [b] Anisotropically refined atoms are given in the form of the isotropic equivalent displacement parameter defined as $B_{eq} = (8\pi^2/3)[a^2B_{11} + b^2B_{22} + c^2B_{33} + ab(\cos\gamma)B_{12} + ac(\cos\beta)B_{13} + bc(\cos\alpha)B_{23}]$. The anisotropic temperature factor expression is $\exp[-2\pi^2(B_{11}a^{*2}h^2 + ... + 2B_{12}a^*b^*hk + ...)]$.

Scheme 1

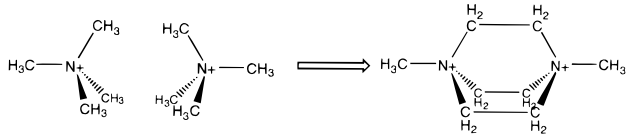

layers of 2-D $[Pd(Se_6)_2]^{2-}$ present very large holes formed by Pd and Se atoms in the form of 28-membered rings. The layers possess a sinusoidal corrugation that propagates along the *b* unit-cell direction; see Figure 2. The organic counterions are placed between these inorganic sheets.

In effect, this compound represents the isolation of the $[Pd(Se_6)_2]^{2-}$ component of K_2PdSe_{10} by replacing the accompanying $[Pd(Se_4)_2]^{2-}$ part (and all the K^+ ions) with the more voluminous $[(CH_3)N(CH_2CH_2)_3N]^+$ cations. The only difference is that the structure of $[Pd(Se_6)_2]^{2-}$ is different (isomeric) from that in K_2PdSe_{10}. The dimensionality of the framework dropped from three to two and probably reflects the fact that this cation may be larger than the optimum size needed

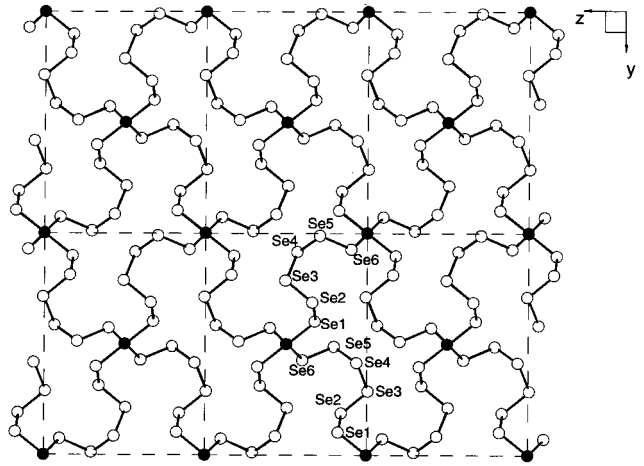

Figure 1. Structure and labeling scheme of the 2-D $[Pd(Se_6)_2]^{2-}$ in **I** looking perpendicular to the layers.

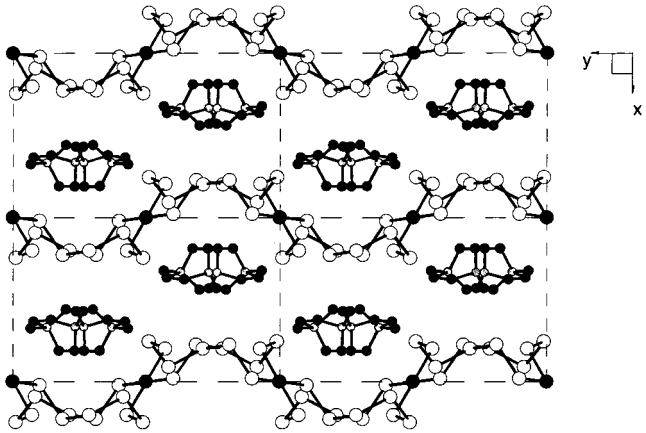

Figure 2. View of $\{(CH_3)N(CH_2CH_2)_3N\}_2[Pd(Se_6)_2]$ (**I**) showing the sinusoidal corrugation of the layers and the location of the organic counterions.

Table 7. Selected Bond Distances (Å) and Angles (deg) for $\{(CH_3)N(CH_2CH_2)_3N\}_2[Pd(Se_6)_2]$[a]

Bond Distances, Å			
Pd−Se(1)	2.464(2)	Se(1)−Se(2)	2.342(3)
Pd−Se(1′)	2.464(2)	Se(2)−Se(3)	2.344(3)
Pd−Se(6)	2.447(2)	Se(3)−Se(4)	2.335(3)
Pd−Se(6′)	2.447(2)	Se(4)−Se(5)	2.346(3)
		Se(5)−Se(6)	2.334(3)
Bond Angles, deg			
Se(1)−Pd−Se(1′)	180.00	Pd−Se(1)−Se(2)	112.2(1)
Se(1)−Pd−Se(6)	88.89(7)	Se(1)−Se(2)−Se(3)	106.1(1)
Se(1)−Pd−Se(6′)	91.11(7)	Se(2)−Se(3)−Se(4)	109.6(1)
Se(1′)−Pd−Se(6)	91.11(7)	Se(3)−Se(4)−Se(5)	108.1(1)
Se(1′)−Pd−Se(6′)	88.89(7)	Se(4)−Se(5)−Se(6)	110.5(1)
Se(6)−Pd−Se(6′)	180.00	Pd−Se(6)−Se(5)	109.7(1)

[a] Standard deviations are given in parentheses.

to fill the void space made available by the $[Pd(Se_4)_2]^{2-}$ framework in K_2PdSe_{10}. Table 7 lists selected bond distances and angles within the $[Pd(Se_6)_2]^{2-}$ sheet; it can be seen that all the Se−Se and Pd−Se bonds are within the normal ranges.

The use of a smaller cation yielded the related but distinct framework compound $(H_3NCH_2CH_2NH_2)_2[Pd(Se_5)_2]$ (**II**). Clearly, the cationic volume has decreased compared to that of the $[(CH_3)N(CH_2CH_2)_3N(CH_3)]^{2+}$ cation above. Here a structural change to a 3-D $[Pd(Se_6)_2]^{2-}$ might be expected, but the system seems to solve the problem of having to contract the anionic volume by decreasing the size of the polyselenide chains by

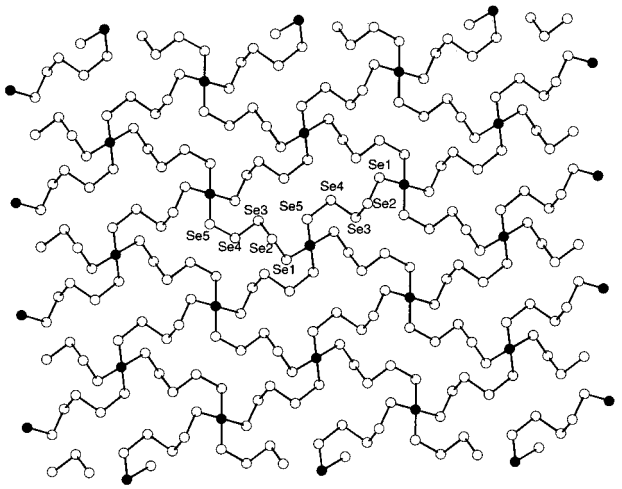

Figure 3. Structure and labeling scheme of the 2-D $[Pd(Se_5)_2]^{2-}$ in **II** looking perpendicular to the layers.

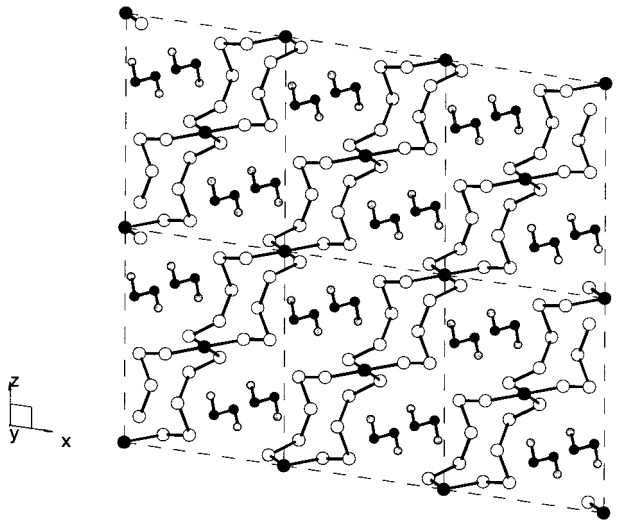

Figure 4. View of $(H_3NCH_2CH_2NH_2)_2[Pd(Se_5)_2]$ (**II**) showing the location of the organic counterions.

Table 8. Selected Bond Distances and Angles for $(H_3NCH_2CH_2NH_2)_2[Pd(Se_5)_2]$[a]

Bond Distances, Å			
Pd−Se(1)	2.450(2)	Se(1)−Se(2)	2.348(3)
Pd−Se(1′)	2.450(2)	Se(2)−Se(3)	2.367(3)
Pd−Se(5)	2.457(2)	Se(3)−Se(4)	2.367(3)
Pd−Se(5′)	2.457(2)	Se(4)−Se(5)	2.358(3)
Bond Angles, deg			
Se(1)−Pd−Se(1′)	180.00	Pd−Se(1)−Se(2)	110.4(1)
Se(1)−Pd−Se(5)	89.95(6)	Se(1)−Se(2)−Se(3)	101.43(9)
Se(1)−Pd−Se(5′)	90.05(6)	Se(2)−Se(3)−Se(4)	103.6(1)
Se(1′)−Pd−Se(5)	90.05(6)	Se(3)−Se(4)−Se(5)	101.9(1)
Se(1′)−Pd−Se(5′)	89.95(6)	Pd−Se(5)−Se(4)	107.25(8)
Se(5)−Pd−Se(5′)	180.00		

[a] Standard deviations are given in parentheses.

one selenium atom. This produced 2-D $[Pd(Se_5)_2]^{2-}$, which now seems to be a good match for the available cation volume. The structure of this two-dimensional net is shown in Figure 3. Given that various Se_x^{2-} species are believed to be present in the synthetic mixtures from which these compounds emerge, the choice of a particular Se_x^{2-} size is controlled exclusively by the system (i.e., low-energy packing possibilities of the various constituents) not the experimenter. In compound **II** the square-planar metal atoms are linked in a slab by Se_5^{2-} units. The 2-D $[Pd(Se_5)_2]^{2-}$ layers, which do not exhibit a corrugation of

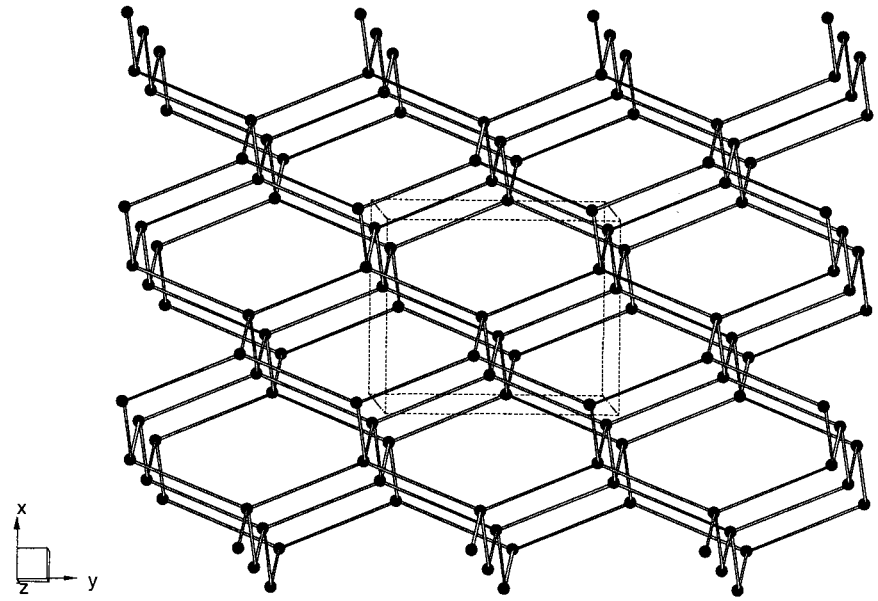

Figure 5. Diamond-like arrangement of Pd atoms in $K_2(H_3NCH_2CH_2NH_3)_2[Pd(Se_4)_2{\cdot}2Se_4]$ (**III**). The Se_4^{2-} bridging ligands have been replaced with lines connecting the metal atoms.

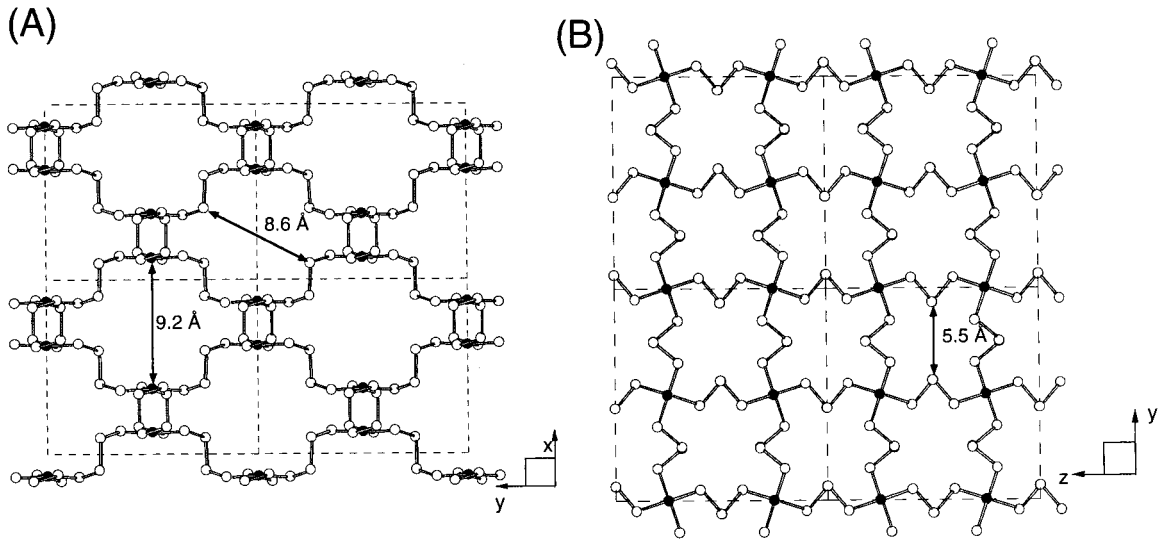

Figure 6. Two views of the structure of the 3-D $[Pd(Se_4)_2]^{2-}$ framework in **III** looking down the *c* axis and *a* axis, respectively. All small molecules and the K^+ ion in the structure have been omitted. The tunnel dimensions are indicated.

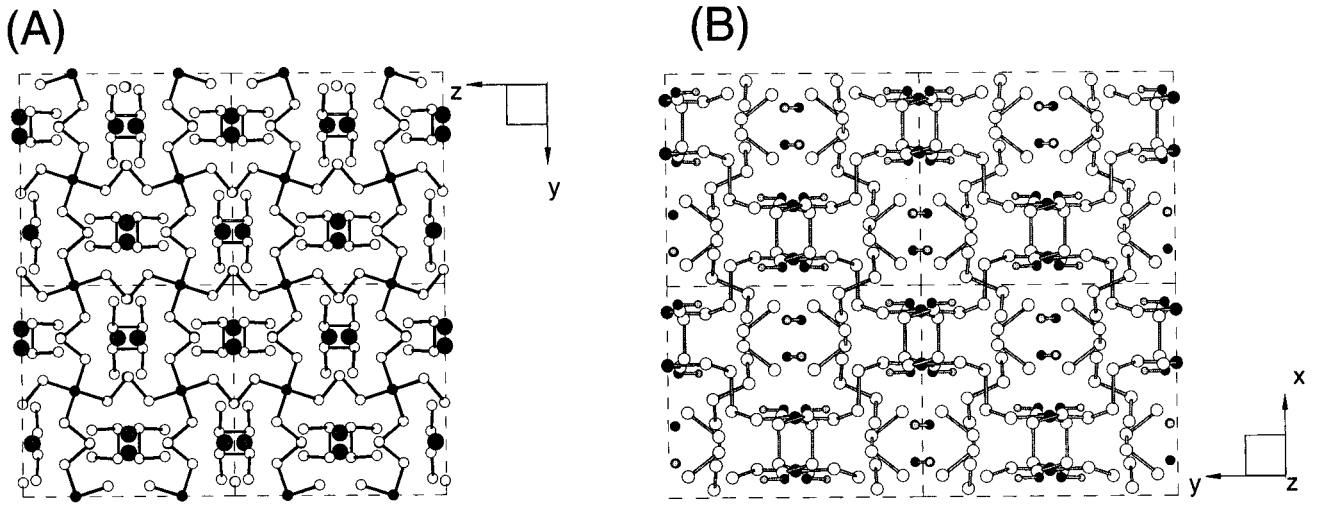

Figure 7. Views of $K_2(H_3NCH_2CH_2NH_3)_2[Pd(Se_4)_2{\cdot}2Se_4]$. (A) The location of the Se_4^{2-} chains and the K^+ atoms are shown (looking down the *a* axis). (B) The $[H_3NCH_2CH_2NH_2]^+$ cations and Se_4^{2-} chains are shown, but the K^+ ions have been omitted for clarity (looking down the *c* axis).

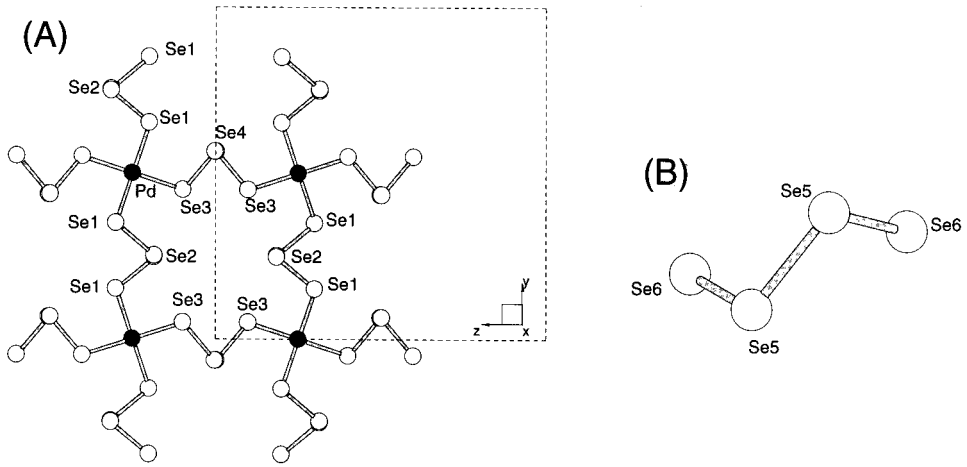

Figure 8. Atomic labeling scheme for the palladium polyselenide framework and the Se_4^{2-} chain in $K_2(H_3NCH_2CH_2NH_3)_2[Pd(Se_4)_2{\cdot}2Se_4]$.

Table 9. Selected Bond Distances and Angles for $K_2(H_3NCH_2CH_2NH_3)_2[Pd(Se_4)_2{\cdot}2Se_4]$[a]

Bond Distances, Å			
Pd−Se(1)	2.438(3)	Se(3)−Se(4)	2.359(5)
Pd−Se(1′)	2.439(3)	Se(4)−Se(4′)	2.36(1)
Pd−Se(3)	2.455(4)	Se(5)−Se(5′)	2.38(1)
Pd−Se(3′)	2.456(4)	Se(5)−Se(6)	2.339(6)
Se(1)−Se(2)	2.361(5)	Se(7)−Se(7′)	2.361(8)
Se(2)−Se(2′)	2.36(1)	Se(7)−Se(8)	2.359(6)

Bond Angles, deg			
Se(1)−Pd−Se(1′)	175.2(2)	Pd−Se(1)−Se(2)	110.0(2)
Se(1)−Pd−Se(3)	90.6(1)	Se(1)−Se(2)−Se(2′)	103.1(2)
Se(1)−Pd−Se(3′)	89.6(1)	Pd−Se(3)−Se(4)	111.0(2)
Se(1′)−Pd−Se(3)	89.6(1)	Se(3)−Se(4)−Se(4′	103.2(2)
Se(1′)−Pd−Se(3′)	90.6(1)	Se(5)−Se(5)−Se(6)	100.9(2)
Se(3)−Pd−Se(3′)	175.4(2)	Se(7′)−Se(7)−Se(8)	101.2(2)

[a] Standard deviations are given in parentheses.

the type observed in 2-D $[Pd(Se_6)_2]^{2-}$ above, also present very large holes formed by Pd and Se atoms in the form of 24-membered rings. It is interesting to note here that the helical-screw conformation of the Se_5^{2-} bridges imposes all the square planes of the Pd atoms to be parallel; see Figure 4. The organic cations are found between these layers. Table 8 lists selected bond distances and angles within the $[Pd(Se_5)_2]^{2-}$ sheet.

Three-Dimensional Systems. The most remarkable structure in this report, however, is that of $K_2[(H_3NCH_2CH_2NH_3)_2[Pd(Se_4)_2{\cdot}2Se_4]$ (**III**), in which, apparently, the selection of two different cations from the reaction medium yields an *effective* average cationic volume that is between that of K^+ and $[H_3NCH_2CH_2NH_2]^+$. This causes the formation of a 3-D $[Pd(Se_4)_2]^{2-}$ framework very much like the one found in K_2PdSe_{10} and with the same diamond-like topology shown in Figure 5. This framework acts as a host for cocrystallized Se_4^{2-} anions. The three-dimensional anion in **III** represents an example of the 3-D $[Pd(Se_4)_2]^{2-}$ framework of K_2PdSe_{10} *removed* from its interpenetrating 3-D $[Pd(Se_6)_2]^{2-}$ framework. Figure 6 shows two views of the empty 3-D $[Pd(Se_4)_2]^{2-}$ framework. The framework possesses large tunnels running along all three crystallographic directions. The tunnel dimensions along the *c* axis are 8.6 Å × 9.2 Å, while down the *a* axis the tunnels are narrower at 5.5 Å; see Figure 6.

The existence of "free", uncoordinated Se_4^{2-} anions in the remaining voids of the lattice as "guest" molecules in **III** is both extraordinary and surprising. This is a rare example of a chalcogenide-based guest−host compound. The three different guest ions (two cations and an anion) and the continuous palladium polyselenide framework constitute an assembly of

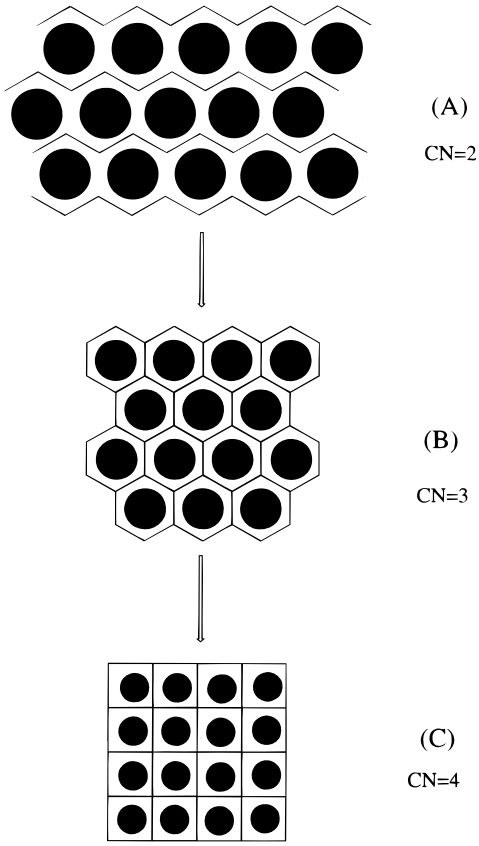

Figure 9. Schematic representation of how chains (A) can be converted to layers (B) via an increase in coordination number as a response to decreasing counterion size. Further decrease of the counterion size results in (C), which is still layered but with increased bonding between the framework atoms. Black spheres represent counterions and thin lines the framework.

stunning complexity. Because of it, a better understanding of the structure can be gained if selected parts of it were displayed in different figures. Figure 7 shows where in the framework its counterions and the guest Se_4^{2-} anions are located. The conformation of the uncoordinated Se_4^{2-} is gauche type with a dihedral angle of ~72°. Selected bond distances and angles for this compound are given in Table 9, while the atomic labeling is given in Figure 8.

The presence of uncoordinated Se_4^{2-} anions suggests the possibility for intracrystal coordination chemistry by introducing transition-metal ions in exchange for K^+ or $[H_3NCH_2CH_2NH_2]^+$

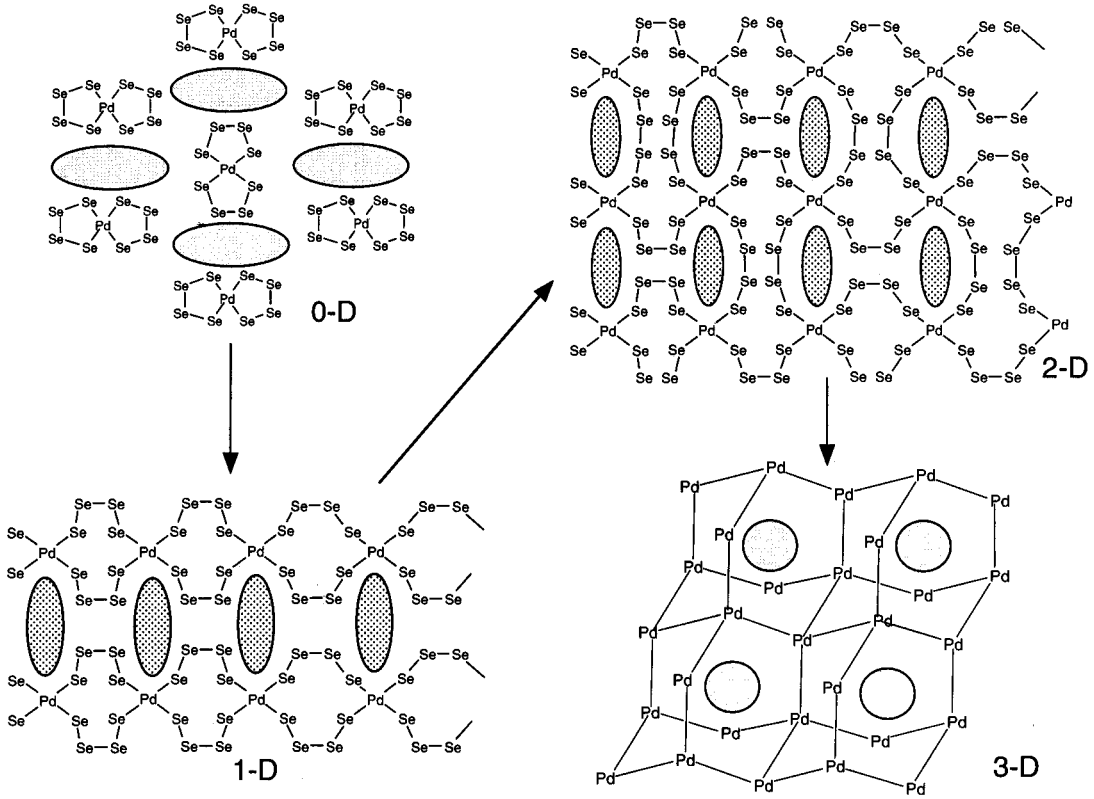

Figure 10. Diagram showing the structural evolution possible when the counterions in a cation/[MSe_x] system become increasingly smaller. In each case a minimum lattice energy must be achieved. Small counterions cannot keep small, discrete anionic molecules well enough apart, and associative interactions may help to retain the anionic composition (i.e., stoichiometry) by forming extended frameworks. Every time a transition occurs from one structure to the next, there is a change in the binding mode of the ligand from chelating to bridging or from one type of bridging to another. This eliminates the repulsive interactions that develop with reduction in cation volume and leads to extended structures of lower lattice energy than the preceding alternative. Excluded from this diagram are, of course, intermediate situations that could arise in the conceptual continuum between 0-D and 3-D phase-space. These would include oligomeric, ladder-type, and multiply associated chains and layers all of which are theoretically possible.

ions so that discrete coordination complexes of the classical kind,[3a,25] $[M(Se_4)_2]^{2-}$ (M = Ni, Zn, Cd, Hg, Pd, etc.), form inside the crystal cavities to give $(H_3NCH_2CH_2NH_3)_2\{Pd(Se_4)_2 \cdot [M(Se_4)_2]\}$.

Remarkably, the crystal lattices of $K_2[(H_3NCH_2CH_2NH_3)_2[Pd(Se_4)_2 \cdot 2Se_4]$ and K_2PdSe_{10} are very similar. Both crystallize in the same space group $I2_12_12_1$ with the former (i.e., **III**) occupying a volume which is ~10% smaller than that of K_2PdSe_{10}. The positioning and conformation of the 3-D $[Pd(Se_4)_2]^{2-}$ framework is almost identical in both compounds. From this we can infer that there is some "breathing" flexibility in the 3-D $[Pd(Se_4)_2]^{2-}$ framework to expand and contract accordingly, which may allow the stabilization of other related compounds with different guest molecules inside. A substantial degree of this flexibility undoubtedly comes from the tortional pliability of the Se_x^{2-} ligands, that is, their ability to vary the Se−Se−Se−Se dihedral angles and alter their shape and spatial extent.

Cation Induced Structural Evolution. In contrast to all salts of $[Pd(Se_x)_2]^{2-}$ mentioned above, the Ph_4P^+ salt stabilizes discrete molecular anions in which two Se_4^{2-} ligands chelate to a single Pd^{2+} atom.[13] To explain the observed differences, one must consider the packing arrangement of anions and cations. In $(Ph_4P)_2[Pd(Se_4)_2]$, it is obvious that the anions and cations pack in such a way as to properly screen each other. When the large Ph_4P^+ cation is changed to the drastically smaller

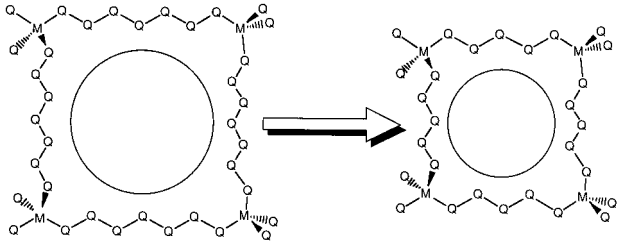

Figure 11. Ring shrinkage through shortening of Se_x^{2-} ligands as a response to a diminishing counterion size. This process changes the stoichiometry but not necessarily the dimensionality of the framework.

$[(CH_3)N(CH_2CH_2)_3N]^+$, $[H_3NCH_2CH_2NH_2]^+$, or K^+, the $[Pd(Se_4)_2]^{2-}$ anions can no longer be effectively screened. This is because they have to pack too close to each other, given that the cationic volume is decreasing while the anionic volume is not, resulting in destabilizing repulsions. If the stoichiometry is to remain the same, the system must respond by decreasing its anionic volume in order to avoid these repulsions. In general, anionic volume can decrease in three different ways. (a) This can be accomplished by a rise in the connectivity of the atoms in the anions (i.e., increased coordination number), which is shown schematically in Figure 9. (b) It could also be achieved through associations of discrete molecules into larger molecules, which could be accomplished by adjustments in the conformations of the various components in the framework. In the case of the Pd/Se_x system, the anionic volume decreases by converting the Se_4^{2-} ligands from chelating one Pd atom to bridging two neighboring Pd atoms, that is association of discrete

(25) (a) Herath-Banda, R. M.; Cusick, J.; Scudder, M. L.; Craig, D. C.; Dance, I. G. *Polyhedron* **1989**, *8*, 1995−1998. (b) Käuter, G.; Ha-Eierdanz, M.-L.; Müller, U.; Dehnicke, K. *Z. Naturforsch.* **1989**, *45b*, 696−700.

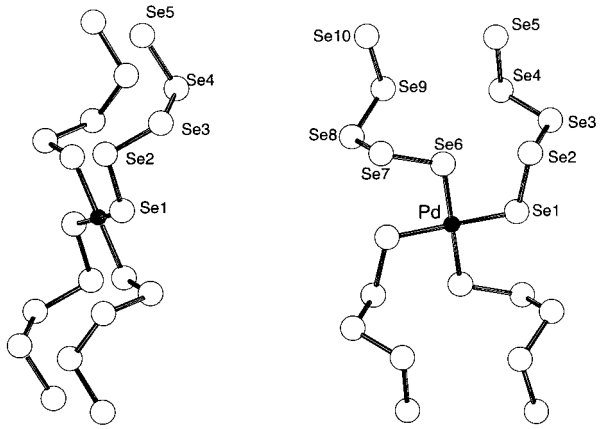

Figure 12. Two views of the $[Pd(Se_5)_4]^{6-}$ anion with the labeling scheme.

molecules. In this fashion the number and type (i.e., metal−Se or Se−Se) of bonds remain constant, with no cost in enthalpy but good gain in lattice energy. This is shown schematically for a generic system in Figure 10. (c) Ejecting atoms from the anion such as ligand shortening (in this case converting Se_6^{2-} to Se_5^{2-} or Se_4^{2-}) would also cause a decrease in anionic volume; see Figure 11. This last option differs from the first two in that it changes the stoichiometry of the compound. Therefore, with this option the system can defer the structural transition, to a higher overall framework dimensionality, until ligand shortening is no longer possible.

The fact that the same anion $[Pd(Se_4)_2]^{2-}$ can be either discrete molecular (when crystallized with Ph_4P^+) or polymeric (when crystallized with K^+) illustrates the magnitude of the influence that the counterion size has in dictating the solid-state structures of complex anionic species. Missing members of the family of compounds described here are the one-dimensional versions of $[Pd(Se_4)_2]^{2-}$, $[Pd(Se_5)_2]^{2-}$, and $[Pd(Se_6)_2]^{2-}$, which may be possible to isolate with the proper size and shape of templating counterions.

The realization that there is a templating effect in the assembly of structures is, of course, instructive. What is significant, however, is the underlined trend associated with this effect *in which decreasing counterion size favors increasing framework connectivity and dimensionality*. This can be well understood in terms of packing considerations and offers a valuable predictive element not only in our comprehension of these systems but also in their deliberate synthetic design. We suspect it is possible to place the counterion effect in more quantitative grounds where appropriate molecular mechanics calculations could more accurately predict the expected structure in any cation/anion system. Such calculations could help select a suitable combination of components in a desired structure.

$K_6[Pd(Se_5)_4]$ (IV): The Precursor? This compound can be isolated from a very basic, highly concentrated solution of K_2Se_x ($4 < x < 6$), and it is slightly water soluble. The ligand concentrations used for its synthesis do not allow the formation of extended structures and stabilize what may very well be the

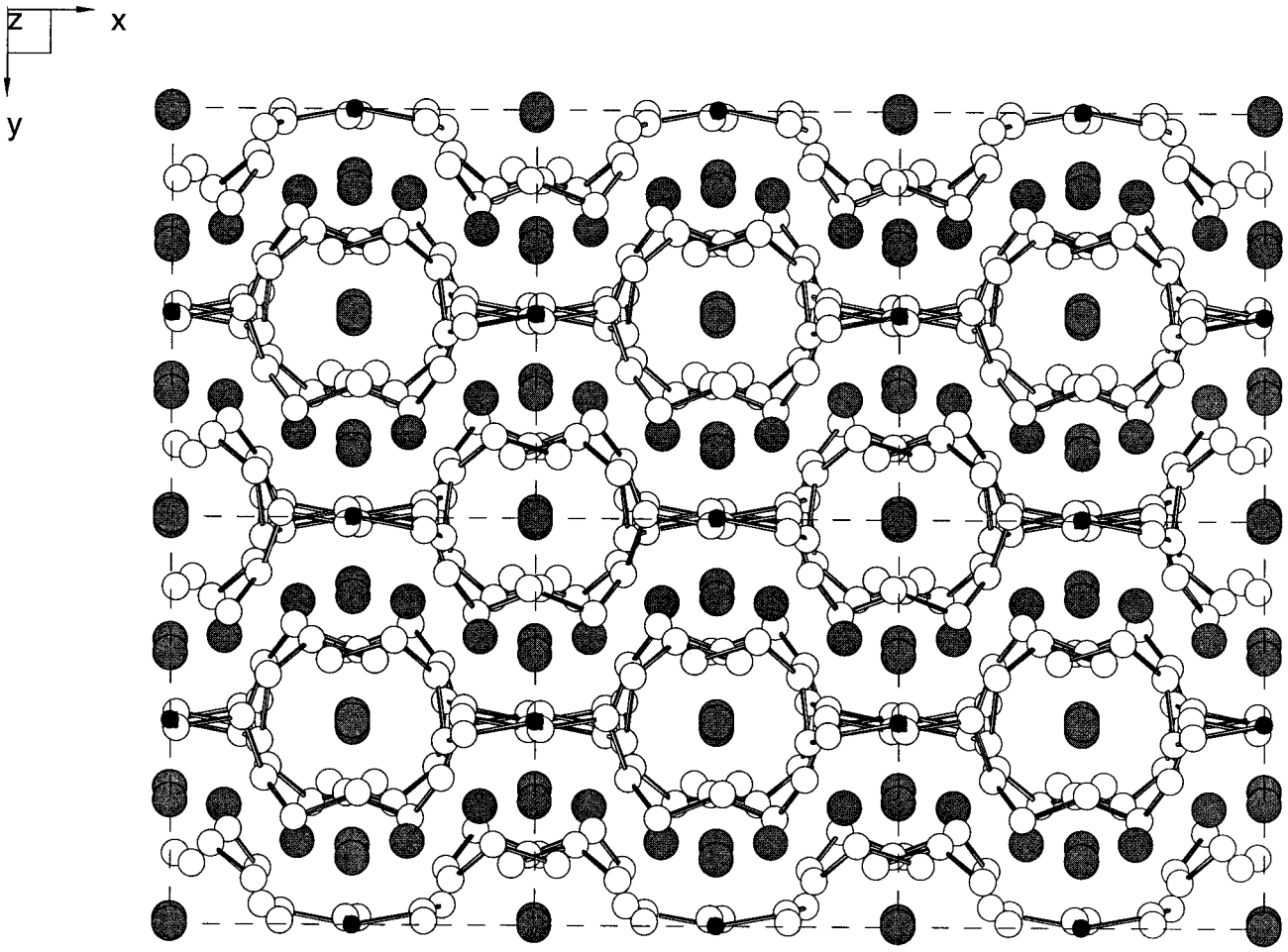

Figure 13. Thee-dimensional organization of K^+ ions and $[Pd(Se_5)_4]^{6-}$ anions in the lattice. Notice the tunnel-forming arrangement of the monodentate Se_5^{2-} ligands at the origin of the unit cell. The packing of $[Pd(Se_5)_4]^{6-}$ anions is lamellar-like, and this requires K^+ ions between the layers of the anions as well as inside the tunnels.

Table 10. Selected Bond Distances and Angles for $K_6[Pd(Se_5)_4]$[a]

Bond Distances, Å			
Pd−Se(1)	2.445(5)	Se(3)−Se(4)	2.362(8)
Pd−Se(1′)	2.445(5)	Se(4)−Se(5)	2.345(7)
Pd−Se(6)	2.457(5)	Se(6)−Se(7)	2.348(7)
Pd−Se(6′)	2.457(5)	Se(7)−Se(8)	2.402(8)
Se(1)−Se(2)	2.371(7)	Se(8)−Se(9)	2.332(8)
Se(2)−Se(3)	2.379(8)	Se(9)−Se(10)	2.327(8)
Bond Angles, deg			
Se(1)−Pd−Se(1′)	180.00	Se(1)−Se(2)−Se(3)	105.7(3)
Se(1)−Pd−Se(6)	90.0(2)	Se(2)−Se(3)−Se(4)	109.9(3)
Se(1)−Pd−Se(6′)	90.0(2)	Se(3)−Se(4)−Se(5)	102.7(3)
Se(1′)−Pd−Se(6)	90.0(2)	Pd−Se(6)−Se(7)	110.8(2)
Se(1′)−Pd−Se(6′)	90.0(2)	Se(6)−Se(7)−Se(8)	107.8(3)
Se(6)−Pd−Se(6′)	180.00	Se(7)−Se(8)−Se(9)	109.1(3)
Pd−Se(1)−Se(2)	110.0(2)	Se(8)−Se(9)−Se(10)	108.5(3)

[a] Standard deviations are given in parentheses.

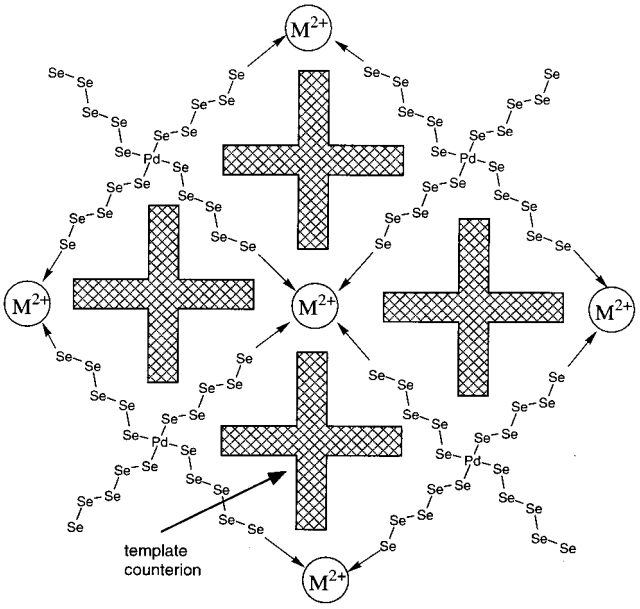

Figure 14. Schematic diagram showing a possible template-induced framework assembly using the $[Pd(Se_5)_4]^{6-}$ anion as a building block via coordination to metal ions. This concept can be used to create novel solid-state heterometallic polychalcogenides.

"precursor" molecule (or one of them) that serves as the fundamental building block for framework construction.

The structure of the $[Pd(Se_5)_4]^{6-}$ anion is related to that of an isoelectronic Au^{3+} complex, $[Au(Se_3)_4]^{5-}$, reported recently, with the only difference being that the former has longer polyselenide ligands.[26] The Pd complex possesses four terminal monodentate Se_5^{2-} ligands arranged in a square-planar fashion around the metal to form one of the most chalcogen-rich compounds ever observed; see Figure 12. This type of metal binding of polychalcogenides is rare, since the chelating mode is more stable. The terminal mode is, of course, forced by the very high ligand concentration. Each Se_5^{2-} chain exhibits a right-handed helical screw-like conformation. Selected bond distances and angles for this complex are given in Table 10.

The anions in $K_6[Pd(Se_5)_4]$ pack in a remarkably well-ordered fashion. The packing view, given in Figure 13, shows how the Se_5^{2-} chains extend away from the Pd atom to form K-filled tunnels parallel to the *c*-axis direction. The cations have naturally aggregated into one-dimensional "pseudochains" parallel to the *c* axis. The selenium atoms from anion to anion

(26) Klepp, K. O.; Weithaler, C. European Meeting on Solid State Chemistry, Montpellier, Sept 1995; Abstract A95.

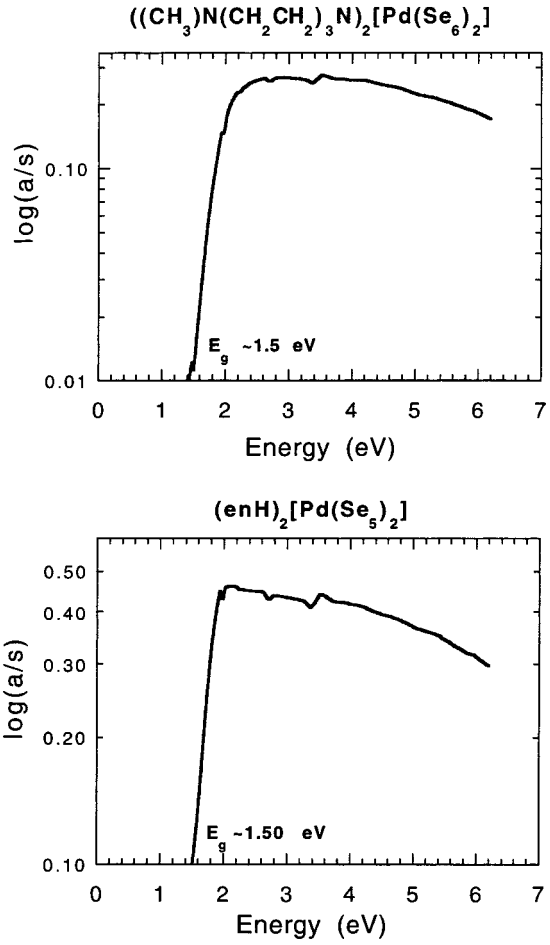

Figure 15. Solid-state optical absorption spectra of $\{(CH_3)N(CH_2CH_2)_3N\}_2[Pd(Se_6)_2]$ (**I**) and $(H_3NCH_2CH_2NH_2)_2[Pd(Se_5)_2]$ (**II**).

maintain a close but nonbonding distance with each other, with the shortest interanion Se−Se distance being ~3.45 Å. This particular proximity of anions suggests merely a packing effect probably driven by the K^+ ions. Despite the lack of interaction, seeing these well-stacked anions makes it easy to envision how extended covalent structures may be derived from such anions. For example, looking at the discrete molecular structure of $[Pd(Se_5)_4]^{6-}$, it is easy to visualize how this species can act as a ligand for additional Pd^{2+} to form binuclear and polynuclear aggregates, which, as they grow, could "wrap around" the available counterions forming open frameworks such as those described above; see Figure 14. This scheme also suggests that a rational route could be set up for the construction of heterobimetallic frameworks if other metals, instead of Pd^{2+}, were used to link the $[Pd(Se_5)_4]^{6-}$ anions. The very high negative charge of $[Pd(Se_5)_4]^{6-}$ suggests that its isolation from ambient temperature conventional solutions would be difficult and underscores the great utility of hydrothermal synthesis even for coordination complexes.

Properties. All compounds, $\{(CH_3)N(CH_2CH_2)_3N\}_2[Pd(Se_6)_2]$ (**I**), $(H_3NCH_2CH_2NH_2)_2[Pd(Se_5)_2]$ (**II**), and $K_2[(H_3NCH_2CH_2NH_3)_2[Pd(Se_4)_2{\cdot}2Se_4]$ (**III**), including $K_2[PdSe_{10}]$, are insoluble in water and various organic solvents such as alcohols, dimethylformamide, acetonitrile, etc. They are all semiconductors with well-defined optical band gaps. It is interesting that the band gaps are relatively insensitive in going from the three-dimensional materials, $K_2[PdSe_{10}]$ at 1.48 eV and $K_2[(H_3NCH_2CH_2NH_3)_2[Pd(Se_4)_2{\cdot}2Se_4]$ at 1.40 eV, to the two-dimensional $(H_3NCH_2CH_2NH_2)_2[Pd(Se_5)_2]$ and $\{(CH_3)N(CH_2CH_2)_3N\}_2[Pd-$

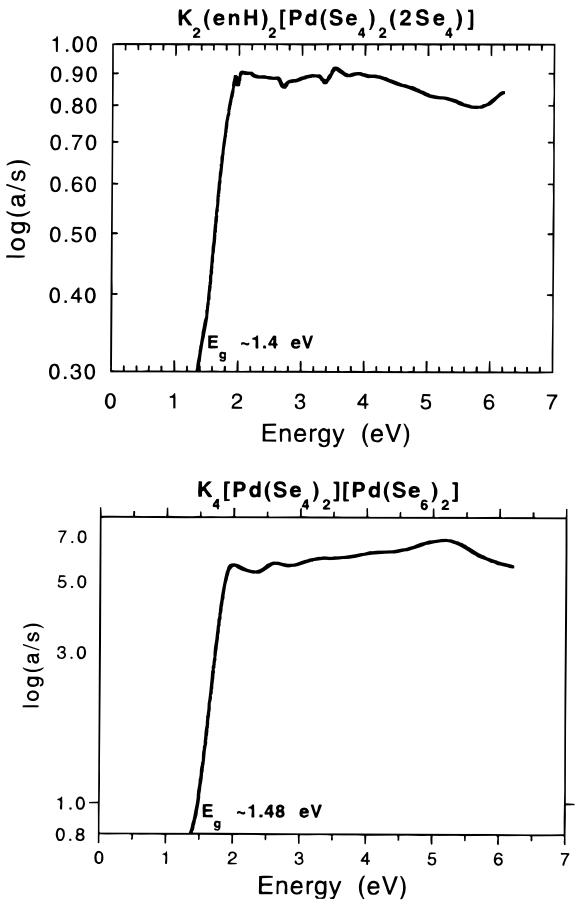

Figure 16. Solid-state optical absorption spectra of $K_2(H_3NCH_2CH_2NH_3)_2[Pd(Se_4)_2{\cdot}2Se_4]$ (**III**) and $K_2[PdSe_{10}]$.

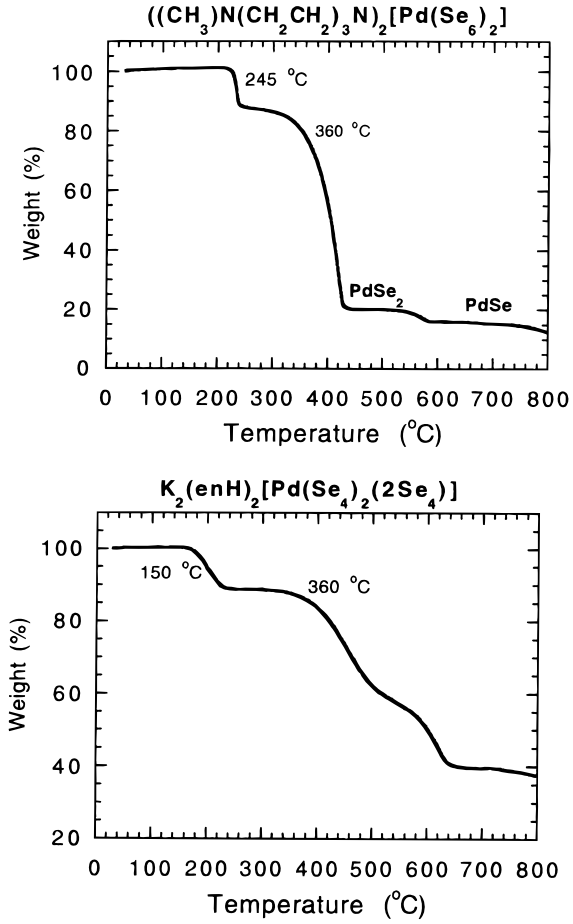

Figure 17. Thermal analysis weight-loss diagrams of $\{(CH_3)N(CH_2CH_2)_3N\}_2[Pd(Se_6)_2]$ (**I**) and $K_2(H_3NCH_2CH_2NH_3)_2[Pd(Se_4)_2{\cdot}2Se_4]$ (**III**). Experiment done under nitrogen flow.

$(Se_6)_2]$ at 1.50 and 1.60 eV, respectively. The onset of the band-gap absorptions seems to be dominated by electronic transitions within the long Se_x^{2-} chains rather than by the nature of the structure or its dimensionality. The solid-state optical absorption spectra of **I**−**III** as well as $K_2[PdSe_{10}]$ are shown in Figures 15 and 16. $K_6[Pd(Se_5)_4]$ shows a solid-state optical spectrum, which features an absorption edge beginning at 1.40 eV.

The thermal stability of the polymeric compounds **I**−**III** was examined with thermal gravimetric analysis (TGA) under nitrogen flow. The materials lose their organic component in a first weight-loss step in the temperature range 150−230 °C, depending on the counterion. The most stable compound is $\{(CH_3)N(CH_2CH_2)_3N\}_2[Pd(Se_6)_2]$, which shows a sharp weight loss at 225 °C followed by a second greater loss step at ∼340 °C; see Figure 17. The weight loss at 340 °C is primarily due to evaporation of elemental selenium and some $CH_3-Se-CH_3$.[27] The final product at 500 °C was shown (with X-ray powder diffraction) to be $PdSe_2$, which in turn slowly converts to PdSe at higher temperatures. Compounds **II** and **III** first lose weight at 200 °C, which is followed by a second weight loss at ∼340 °C.

$K_2[(H_3NCH_2CH_2NH_3)_2[Pd(Se_4)_2{\cdot}2Se_4]$ loses its ethylenediamine molecule at 150 °C, and this event is followed by another weight loss beginning at 360 °C. The latter is associated with evaporation of H_2Se and elemental Se leaving behind a residue of $PdSe_2$ and an unidentified K/Pd/Se phase. It would be interesting to fully characterize the product obtained after the evolution of the ethylenediamine from the structure and before the second weight loss at 360 °C.

(27) Detected by mass spectrometry.

Concluding Remarks

The existence of the various cation/Pd/Se_x architectures described here demonstrates the considerable flexibility of these systems to adapt to changing counterions in such a way as to form higher-dimensional structures with decreasing counterion size. The Pd system seems to be particularly amenable to this kind of manipulation. Undoubtedly, there are many more anionic Pd/Se_x framework materials to be built by judiciously varying the templating counterions.[28] We point out, however, that other metal/Se_x systems seem equally amenable to this type of stratagem. A lot can be learned regarding the factors which are important in controlling the structure, dimensionality, and perhaps stoichiometry of the particular framework by doing so. These lessons may be useful in qualitatively predicting or designing frameworks of this type in many classes of materials. Finally, it should be possible to use computational techniques to match proper counterions and Pd/Se_x and M/Se_x frameworks and make more quantitative predictions of structure and stability in such compounds.

Acknowledgment. Financial support from the National Science Foundation Grant CHE 96-33798 (Chemistry Research Group) and from the donors of the Petroleum Research Fund administered by the American Chemical Society is gratefully acknowledged. This work made use of the SEM facilities of

(28) (a) Recently, we bacame aware that the Cs_2PdSe_8 also has a single three-dimensional polymeric framework, and it too belongs to the greater family of materials described in the present publication. (b) Li, J.; Chen, Z.; Wang, R.-J.; Lu, J. Y. Submitted.

the Center for Electron Optics, Michigan State University. M.G.K. is a Henry Dreyfus Teacher Scholar 1993−1998.

Supporting Information Available: Tables of calculated and observed X-ray powder diffraction patterns, positional and anisotropic thermal parameters of all atoms, and bond distances and angles for **I**−**IV** (24 pages, print/PDF). See any current masthead page for ordering information and web access instructions.

JA981297S